

## 32. A Long Wave in the Vicinity of an Estuary [VII].

### — Case of Outflow —

By Takao MOMOI,

Earthquake Research Institute.

(Read May 26, 1970.—Received May 30, 1970.)

#### Abstract

In order to examine the behavior of trapping waves in a rectangular bay, the long wave around the estuary for the outflowing wave is discussed focussing our attention upon the reflexion coefficient. The theory developed is a rigorous one based on the buffer domain method.

#### 1. Introduction

Succeeding the previous works (Momoi, 1965a—1969), the long wave around the estuary is discussed for the case of periodic waves incident upon the estuary from the inside of the canal. The primary purpose of this paper is to examine the reflection coefficient of the reflected wave to the outflowing (incident) wave. The reflection rate is of much benefit to the study of the trapping wave in a rectangular bay which will be made in the future.

#### 2. Rigorous Theory

In this section rigorous solution is presented on the basis of the buffer domain method.

##### 2.1. Model used.

An entire portion of waters is assumed to have a uniform depth. Referring to Fig. 1, the origin of the coordinate is located at the midpoint of the estuary, the  $x$ - and  $y$ -axes being taken along the coastline facing the open sea and along the axis of the canal with breadth  $2d$ . A train of periodic waves

$$\zeta_{in} = e^{-i\omega t +iky} \quad (1)$$

is then propagated from the inside of the

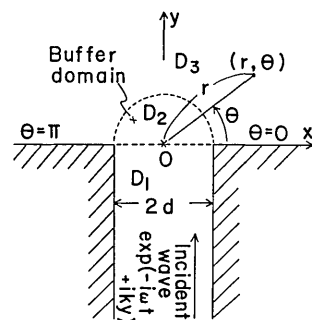


Fig. 1. Model used.

canal toward the open sea, where  $\omega$  and  $t$  are the angular frequency and time variable.

### 2.2. Equation and Conditions.

Basic equation for periodic waves is given by

$$\left(\frac{\partial^2}{\partial x^2} + \frac{\partial^2}{\partial y^2} + k^2\right)\zeta = 0, \quad (2)$$

where

$\zeta$ : the wave height,  
 $k$ : the wave number.

Conditions at the rigid boundary are

$$\left. \begin{aligned} \frac{\partial \zeta}{\partial x} = 0 & \quad \text{at } (|x|=d, y < 0), \\ \frac{\partial \zeta}{\partial y} = 0 & \quad \text{at } (|x| > d, y = 0). \end{aligned} \right\} \quad (3)$$

### 2.3. Formal Expressions.

Let the domain separate into three parts as shown in Fig. 1, i e,

$D_1$ : the domain in the range  $(|x| < d, y < 0)$ ,  
 $D_2$ : the domain in the range  $(r < d, 0 < \theta < \pi)$ ,  
 $D_3$ : the domain in the range  $(r > d, 0 < \theta < \pi)$ ,

where  $(r, \theta)$  are the polar coordinate.

Allowing for boundary condition (3), the formal solutions are expressed as follows.

$$\zeta_1 = e^{iky} + \sum_{n=0}^{\infty} \zeta_1^{(n)} e^{-i(kn)y} \cos \frac{n\pi}{d} x \quad (4)$$

in domain  $D_1$ ,

$$\zeta_2 = \sum_{n=0}^{\infty} \{\zeta_2^{(2n)} J_{2n}(kr) \cos 2n\theta + \zeta_2^{(2n+1)} J_{2n+1}(kr) \sin (2n+1)\theta\} \quad (5)$$

in domain  $D_2$ ,

and

$$\zeta_3 = \sum_{n=0}^{\infty} \zeta_3^{(2n)} H_{2n}^{(1)}(kr) \cos 2n\theta \quad (6)$$

in domain  $D_3$ ,

where

$$(kn) = k_n = \sqrt{k^2 - \left(\frac{n\pi}{d}\right)^2}$$

and  $\zeta_1^{(n)}$ ,  $\zeta_2^{(2n)}$ ,  $\zeta_2^{(2n+1)}$ ,  $\zeta_3^{(2n)}$  are the unknown factors to be determined by the conditions between the adjacent domains.

2.4. Infinite Simultaneous Equations.

In order to determine the unknown factors in expressions (4) to (6), the boundary conditions

$$\left. \begin{aligned} \zeta_2 &= \zeta_1 \\ \frac{\partial \zeta_2}{\partial y} &= \frac{\partial \zeta_1}{\partial y} \end{aligned} \right\} \text{ at } y=0 \tag{7}$$

and

$$\left. \begin{aligned} \zeta_2 &= \zeta_3 \\ \frac{\partial \zeta_2}{\partial r} &= \frac{\partial \zeta_3}{\partial r} \end{aligned} \right\} \text{ at } r=d \tag{8}$$

are available.

Applying operator

$$\int_0^d \cos \frac{m\pi}{d} x dx \quad (m=0, 1, 2, \dots)$$

to (7) after substitution of (4) and (5), we have

$$\sum_{n=0}^{\infty} \left\{ \begin{aligned} \zeta_2^{(2n)} K'_{n,m} \\ \zeta_2^{(2n+1)} L'_{n,m} \end{aligned} \right\} - \varepsilon_m \zeta_1^{(m)} \left\{ \begin{aligned} kd \\ (-ik_m d) \end{aligned} \right\} = \varphi_m \left\{ \begin{aligned} kd \\ ikd \end{aligned} \right\} \quad (m=0, 1, 2, \dots), \tag{9}$$

where

$$\left. \begin{aligned} \varphi_m &= 1 \quad (m=0) \\ &= 0 \quad (m \neq 0) \end{aligned} \right\}, \quad \left. \begin{aligned} \varepsilon_m &= 1 \quad (m=0) \\ &= 1/2 \quad (m \neq 0) \end{aligned} \right\},$$

and

$$\left. \begin{aligned} K'_{n,m} &= \int_0^{kd} J_{2n}(z) \cos \frac{m\pi}{kd} z dz, \\ L'_{n,m} &= (2n+1) \int_0^{kd} \frac{J_{2n+1}(z)}{z} \cos \frac{m\pi}{kd} z dz. \end{aligned} \right\}$$

Likewise, applying operator

$$\int_0^\pi \cos 2m\theta d\theta \quad (m=0, 1, 2, \dots)$$

to (8) after substitution of (5) and (6), we have

$$\zeta_2^{(2m)} \begin{Bmatrix} J_{2m} \\ J'_{2m} \end{Bmatrix} + \frac{2}{\varepsilon_m \pi} \sum_{n=0}^{\infty} I_{m, n} \begin{Bmatrix} J_{2n+1} \\ J'_{2n+1} \end{Bmatrix} \zeta_2^{(2n+1)} = \zeta_3^{(2m)} \begin{Bmatrix} H_{2m}^{(1)} \\ H_{2m}^{(1)'} \end{Bmatrix} \quad (m=0, 1, 2, \dots), \quad (10)$$

where

$$J_\nu = J_\nu(kd), \quad J'_\nu = J'_\nu(kd), \quad H_\nu^{(1)} = H_\nu^{(1)}(kd), \\ H_\nu^{(1)'} = H_\nu^{(1)'}(kd) \quad (\nu: \text{order of Bessel function})$$

and

$$I_{m, n} = \frac{2n+1}{(2n+1)^2 - (2m)^2}.$$

Eliminations of  $\zeta_1^{(m)}$  and  $\zeta_3^{(2m)}$  from (9) and (10) yield

$$i \cdot \frac{k_m d}{kd} \sum_{n=0}^{\infty} \zeta_2^{(2n)} K'_{n, m} + \sum_{n=0}^{\infty} \zeta_2^{(2n+1)} L'_{n, m} = \varphi_m \cdot 2ikd \quad (m=0, 1, 2, \dots) \quad (11)$$

and

$$\varepsilon_m \zeta_2^{(2m)} - ikd \sum_{n=0}^{\infty} I_{m, n} (J_{2n+1} H_{2m}^{(1)'} - J'_{2n+1} H_{2m}^{(1)}) \zeta_2^{(2n+1)} = 0 \quad (m=0, 1, 2, \dots). \quad (12)$$

Equations (11) and (12) are final forms to be obtained in this section.

### 2.5. Reduction to Finite Simultaneous Equations.

Setting down

$$\left. \begin{aligned} J_m(kr) &\cong 0 & (m \leq 2l+1) \\ J_m(kr) &\equiv 0 & (m > 2l+1) \end{aligned} \right\} \text{for } r < d, \quad (13)$$

equations (11) and (12) are reduced to the following.

$$i \cdot \frac{k_m d}{kd} \sum_{n=0}^l X_{n+1} K_{n, m} + \sum_{n=0}^l X_{l+2+n} L_{n, m} = \varphi_m \cdot 2ikd \quad (m=0, 1, 2, \dots, l) \quad (14)$$

and

$$\frac{\varepsilon_m}{J_{2m} H_{2m}^{(1)'}} X_{m+1} - ikd \sum_{n=0}^l I_{m, n} \left( 1 - \frac{J'_{2n+1} H_{2m}^{(1)}}{J_{2n+1} H_{2m}^{(1)'}} \right) X_{l+2+n} = 0 \quad (m=0, 1, 2, \dots, l), \quad (15)$$

where

$$\left. \begin{aligned} X_{n+1} &= \zeta_2^{(2n)} J_{2n}, \\ X_{l+2+n} &= \zeta_2^{(2n+1)} J_{2n+1} \end{aligned} \right\} \quad (16)$$

and

$$\left. \begin{aligned} K_{n,m} &= \frac{1}{J_{2n}} \int_0^{kd} J_{2n}(z) \cos \frac{m\pi}{kd} z dz, \\ L_{n,m} &= \frac{(2n+1)}{J_{2n+1}} \int_0^{kd} \frac{J_{2n+1}(z)}{z} \cos \frac{m\pi}{kd} z dz. \end{aligned} \right\} \quad (17)$$

With a view to avoiding the accumulation of truncation error on the electronic computer, coefficients of equation (14) are normalized by factors  $J_{2n}$  and  $J_{2n+1}$ , those of equation (15) by  $J_{2m} H_{2m}^{(1)'}$  and  $J_{2n+1} H_{2m}^{(1)'}$ .

Solving equations (14) and (15), unknown factors

$$\zeta_2^{(m)} \quad (m=0, 1, 2, \dots, 2l+1) \quad (18)$$

in domain  $D_2$  begin to be known through expression (16). In calculation of integral (17) Filon's method is employed, of which the procedure is detailed in Section 2 of the fifth work (Momoi, 1968b).

Substitution of (18) into the first expressions of (9) and (10) gives the values of

$$\zeta_1^{(m)} \text{ and } \zeta_3^{(2m)} \quad (m=0, 1, 2, \dots). \quad (19)$$

Behaviors of the wave around the estuary can now be elucidated through use of formal expressions (4) to (6) with substitution of (18) and (19).

### 3. Approximated Theory

In this section, development of the approximated theory is done for  $2d \ll L$  ( $2d$ : width of the canal,  $L$ : wave-length). The model used is completely the same as that in Section 2. In the analysis of this section the incident wave is expressed by

$$F_{in} = e^{+i\omega t - iky} \quad (20)$$

instead of  $e^{-i\omega t + iky}$  in the previous section. Under the approximation  $2d \ll L$ , higher modes of the wave in the canal are neglected. Following the same procedure as those developed by Ippen-Goda (Ippen-Goda, 1963), Mitsui (Mitsui, 1966) and Momoi (Momoi, 1970), the analysis is carried out.

Basic equation and boundary conditions are given by (2) and (3).

The entire domain is separated into two parts, i. e.,

$D_1$ : the domain in the range ( $|x| < d$ ,  $y < 0$ ),

$D_3$ : the domain in the range ( $-\infty < x < \infty$ ,  $y > 0$ ),

in place of three domains in Section 2. For the geometry of the domains and nomenclature, Fig. 2 should be referred to.

Using expression (20), wave heights  $F_j$  in domains  $D_j$  ( $j=1,3$ ) are expressed as

$$F_1 = e^{-iky} + Re^{+iky} \quad (21)$$

and

$$F_3 = \chi(x, y). \quad (22)$$

In the above,  $R$  is the complex reflexion coefficient. After the procedure by Ippen-Goda, Mitsui or Momoi, we have

$$R = \frac{2iI - \pi}{2iI + \pi} \quad (23)$$

and

$$\chi(x, y) = Q \cdot \int_0^\infty \frac{\sin \xi}{\xi \gamma} e^{-\gamma y/d} \cos(\xi x/d) d\xi, \quad (24)$$

where

$$I = kd \int_0^\infty \frac{\sin^2 \xi}{\xi^2 \gamma} d\xi, \quad (25)$$

$$\gamma = \sqrt{\xi^2 - (kd)^2}, \quad Q = \frac{4ikd}{2iI + \pi}.$$

#### 4. Numerical Calculation

Computational aspects are given in this section.

##### 4.1. Validity of Our Theory.

Validity of the rigorous theory developed in Section 2 is ascertained through the calculation of the reflexion coefficient of the approximated theory in Section 3. The reflexion coefficient of the rigorous theory is given by  $\zeta_1^{(0)}$  in expression (4) and that of the approximated theory by (23). The calculated results are presented in Fig. 3. According to the figure, the absolute value of the reflexion coefficients of two theories is in very good agreement up to  $kd \approx 2.0$ . In calculation of integral (25), Simpson's formula is employed.

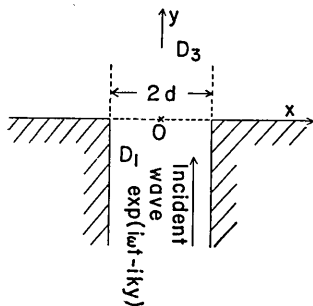


Fig. 2. Nomenclature of the model used for  $2d \ll L$ .

4.2. Reflexion Coefficient and the First Mode.

The calculated value of reflexion coefficient  $\zeta_1^{(0)}$  is arranged in Table 1 for  $kd$  in the range 0 to 3.14 ( $\approx \pi$ ), of which the variation is shown in Fig. 3 with the curve of the first mode  $|\zeta_1^{(1)}|$ . According to Table 1,  $|\zeta_1^{(0)}|$  decreases monotonically from 1.0 with increase of  $kd$  to lessen down to the value below 0.1 in the range  $kd > 2.0$ , while  $\arg \zeta_1^{(0)}$  has  $-\pi$  for  $kd=0$  to decrease in absolute value with increase of  $kd$ .

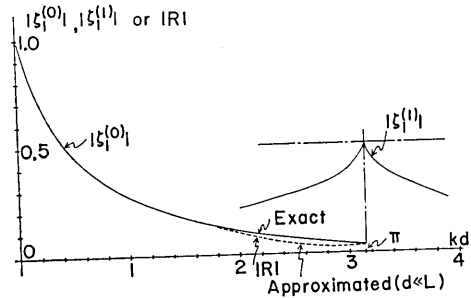


Fig. 3. Amplitude variation of each mode of the reflected wave in the canal. The solid lines denote  $|\zeta_1^{(0)}|$  and  $|\zeta_1^{(1)}|$  of the rigorous theory, the broken line the reflexion coefficient  $|R|$  of the approximated theory ( $d \ll L$ ).

Table 1. Reflexion coefficient  $\zeta_1^{(0)}$  at the estuary (KD, AB and PH denote, respectively  $kd$ ,  $|\zeta_1^{(0)}|$  and  $\arg \zeta_1^{(0)}$ )

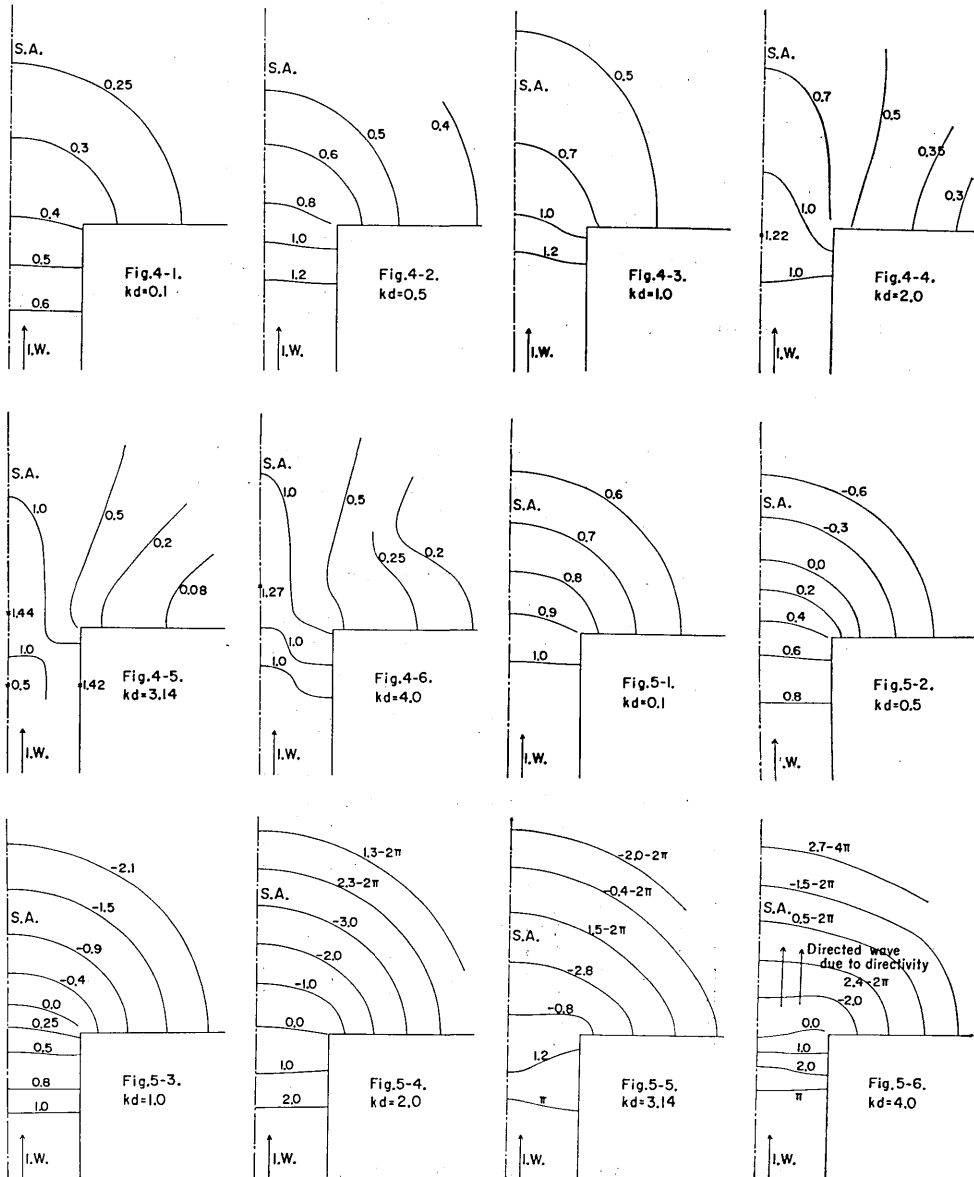
KD= 0.050	AB= 0.90618	PH=-2.89447
KD= 0.060	AB= 0.88898	PH=-2.85913
KD= 0.080	AB= 0.85609	PH=-2.79462
KD= 0.100	AB= 0.82514	PH=-2.73655
KD= 0.200	AB= 0.69520	PH=-2.50780
KD= 0.300	AB= 0.59673	PH=-2.33842
KD= 0.400	AB= 0.51933	PH=-2.20135
KD= 0.500	AB= 0.45762	PH=-2.08721
KD= 0.600	AB= 0.40689	PH=-1.98623
KD= 0.800	AB= 0.32757	PH=-1.81670
KD= 1.000	AB= 0.26802	PH=-1.67785
KD= 1.200	AB= 0.22162	PH=-1.56070
KD= 1.400	AB= 0.18445	PH=-1.46136
KD= 1.600	AB= 0.15401	PH=-1.37925
KD= 1.800	AB= 0.12878	PH=-1.31437
KD= 2.000	AB= 0.10770	PH=-1.26779
KD= 2.200	AB= 0.08790	PH=-1.27474
KD= 2.400	AB= 0.07317	PH=-1.31877
KD= 2.600	AB= 0.06118	PH=-1.29857
KD= 2.800	AB= 0.05054	PH=-1.39363
KD= 3.000	AB= 0.04261	PH=-1.53272
KD= 3.140	AB= 0.03697	PH=-1.94934

This table is the result of the computer output.

As for the first mode of the reflected wave, the amplitude  $|\zeta_1^{(1)}|$  takes a maximum value at  $kd=\pi$ , which amounts to 0.5.  $kd=\pi$  refers to the resonance of the first mode of waves in the canal.

4.3. RST Wave.

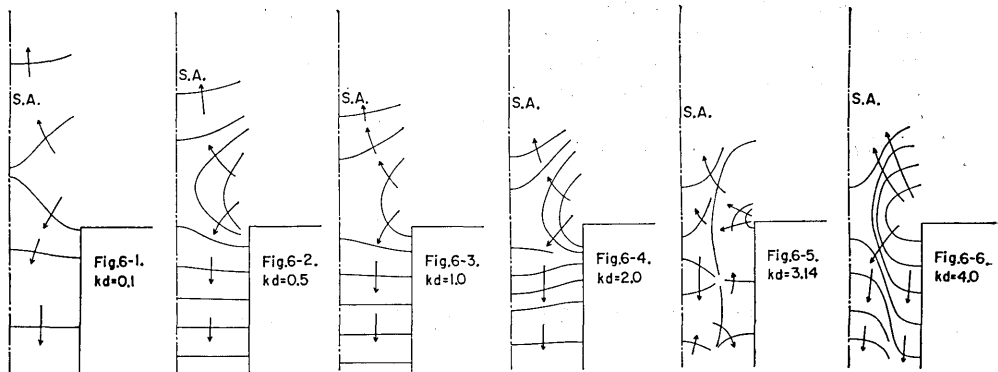
RST wave is the abbreviation of resultant wave. RST wave is calculated by the procedure described in Section 2. In the calculation, the degree of the approximation  $(2l+1)$  is taken large enough to keep



Figs. 4-1 to 4-6. Amplitude variations of RST wave\*.  
 Figs. 5-1 to 5-6. Phase variations of RST wave\*.

\* I.W. and S.A. are the abbreviations of "incident wave" and "symmetric axis".

good convergence. The calculated results are presented in Figs. 4-1 to 4-6 for the amplitude and in Figs. 5-1 to 5-6 for the phase. The computed range of  $kd$  is 0.1 to 4.0. According to these figures, the following facts are exposed. The outflowing wave in the open sea is small in amplitude for small  $kd$  (see Figs. 4-1 to 4-3) as a result of the strong reflection toward the inside of the canal, while, as  $kd$  increases, the above amplitude begins to be large, of which the value approaches a unit showing the aspect of elongation toward the open sea due to the strong directivity of the wave. The lastly stated behavior of the directivity of the wave is also perceived in Figs. 5-1 to 5-6.



Figs. 6-1 to 6-6. Phase variation of the reflected wave\*.

4.4. Reflected Wave.

The wave reflected at the estuary ( $\zeta_{ref}$ ) can be discussed by the procedure

$$\zeta_{ref} = \zeta_{rst} - e^{+iky}$$

where  $\zeta_{rst}$  is the wave height of RST wave obtained in Section 2 and  $e^{+iky}$  the incident wave. The computation is carried out for the phase of the value  $kd=0.1$  to 4.0 and for the amplitude of  $kd=3.14$ . The results are presented in Figs. 6-1 to 6-6 for the phase and in Fig. 7 for the amplitude. In Figs. 6-1 to 6-6, the wave is reflected definitely from the corner of the estuary. In order to examine the amplitude of the resonating wave, the amplitude variation of the reflected wave is depicted only for the value of  $kd=3.14$  ( $\approx \pi$ ). According to Fig. 7, the loop and node run along the axis of

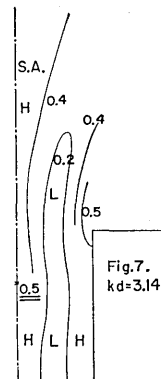


Fig. 7. Amplitude variation of the reflected wave for a specified value of  $kd \approx \pi^*$ .

\* See the footnote of Figs. 4-1 to 4-6.

the canal suggesting the excitation of the resonating lateral wave. The excitation amounts to 0.5 in amplitude (see the value with double underlines in Fig. 7), of which the value is the same as that found for the case of normal invasion of the incident wave from the open sea (see Section 4 of the sixth paper (Momoi, 1969)).

### References

- IPPEN, A. I. and Y. GODA, 1963, Wave induced Oscillations in Harbours, *Hydrodynamics Labo. Rep. No. 59, MIT*, 5 and 21.
- MITSUI, H., 1966, Distribution of Wave Heights along Harbor and Coastal Structures with Discontinuous Alignments (Part 1), *Proc. 13th CEC, JSCE*, 80-86.
- MOMOI, T., 1965a, 1965b, 1966, 1968a, 1968b and 1969, A Long Wave in the Vicinity of an Estuary [I], [II], [III], [IV], [V] and [VI], *Bull. Earthq. Res. Inst.*, **43**, **43**, **44**, **46**, **46** and **47**, 291-316, 459-498, 1009-1040, 631-650, 1237-1268 and 487-521.
- MOMOI, T., 1970, A Long Wave around a Breakwater with Finite Thickness [I], *Bull. Earthq. Res. Inst.*, **48**, 613-635.

---

## 32. 河口近傍における長波について [VII]

### — 流出波の場合 —

地震研究所 桃井高夫

本報告においては河口水路より波が流出する場合が論じられている。ここでは主として矩形の湾における長波の状態を調べるのに使用する反射係数に集点を合せて論を展開している。解は buffer domain の方法による厳密解である

---